

# Diffusion and Home Range Parameters for Rodents: *Peromyscus maniculatus* in New Mexico

G. Abramson<sup>a,b</sup>, L. Giuggioli<sup>a</sup>, V. M. Kenkre<sup>a</sup>

<sup>a</sup>*Consortium of the Americas for Interdisciplinary Science, University of New Mexico, Albuquerque, New Mexico 87131, USA.*

<sup>b</sup>*Centro Atómico Bariloche, CONICET and Instituto Balseiro, 8400 San Carlos de Bariloche, Río Negro, Argentina.*

J. W. Dragoo, R. R. Parmenter, C. A. Parmenter, T. L. Yates

*Department of Biology, University of New Mexico, Albuquerque, New Mexico 87131, USA.*

---

## Abstract

We analyze data from a long term field project in New Mexico, consisting of repeated sessions of mark-recaptures of *Peromyscus maniculatus* (Rodentia: Muridae), the host and reservoir of Sin Nombre Virus (Bunyaviridae: Hantavirus). The displacements of the recaptured animals provide a means to study their movement from a statistical point of view. We extract two parameters from the data with the help of a simple model: the diffusion constant of the rodents, and the size of their home range. The short time behavior shows the motion to be approximately diffusive and the diffusion constant to be  $470 \pm 50 \text{ m}^2/\text{day}$ . The long time behavior provides an estimation of the diameter of the rodent home ranges, with an average value of  $100 \pm 25 \text{ m}$ . As in previous investigations directed at *Zygodontomys brevicauda* observations in Panama, we use a box model for home range estimation. We also use a harmonic model in the present investigation to study the sensitivity of the conclusions to the model used and find that both models lead to similar estimates.

*Key words:* Peromyscus, animal diffusion, rodents, home range, Hantavirus

---

*Email addresses:* abramson@cab.cnea.gov.ar (G. Abramson), giuggioli@unm.edu (L. Giuggioli), kenkre@unm.edu (V. M. Kenkre), jdragoo@unm.edu (J. W. Dragoo), bparmenter@vallescaldera.gov (R. R. Parmenter), cparment@sevilleta.unm.edu (C. A. Parmenter), tyates@unm.edu (T. L. Yates).

## 1 Introduction and Estimated Results

Since the discovery of Sin Nombre Virus (Bunyaviridae: Hantavirus) in 1993 as the agent of the severe Hantavirus Pulmonary Syndrome (HPS) in the North American Southwest (Nichol et al., 1993), a continuing effort is being maintained to study the long-term dynamics of its principal host, the deer mouse, *Peromyscus maniculatus* (Childs et al., 1994). As part of this effort, an analytical model (Abramson and Kenkre, 2002; Abramson et al., 2003) has been developed and has led to an understanding of spatio-temporal patterns that have been observed in the field. A basic assumption of that model is that the rodent movement may be regarded as diffusive and characterized by a parameter  $D$ , the diffusion coefficient. Various contributions to the understanding of animal movement in general (Okubo, 1979; Murray, 1993), as well specific considerations for *Peromyscus* (Stickel, 1968; Vessey, 1987), form the background of this hypothesis. The present paper is one in a series of investigations which have been launched to assess the validity of the assumption of diffusive movement and to extract the parameter  $D$  from field observations.

In the first paper in the series (Giuggioli et al., 2005a), hereafter referred to as I, field data for *Zygodontomys brevicauda* in Panama were used to obtain  $D$  from trapping measurements in a grid arrangement. During that investigation, a procedure was given to deduce an *additional* parameter of the rodent motion:  $L$  the home range size. It was found that  $D \sim 200 \text{ m}^2/\text{day}$  and  $L \sim 70 \text{ m}$ . Here we express the home range size as a length rather than an area.

It is important to extract such parameters in different real scenarios. One reason is to extend our knowledge about different animals involved in the spread of the epidemic, the second to gain a thorough understanding of the underlying theory. In the present paper, we investigate a system that differs from that analyzed in I in three characteristics: the rodent, the region, and the method of measurement. The rodent is *Peromyscus maniculatus*, the region is New Mexico (USA), and the measurement method is trapping in the web arrangement (Parmenter et al., 2003). As will be seen below, we find for the present system that short time measurements show the diffusion constant to be  $D = 470 \pm 50 \text{ m}^2/\text{day}$  while the long time measurements show the home range size to be  $L = 100 \pm 25 \text{ m}$ <sup>\*</sup>. The latter is a consequence of using the box model introduced in I for home range estimation. An additional question we raise in the present paper concerns the sensitivity of the home range estimation to the precise assumptions of the model. By using a harmonic potential (instead of

---

<sup>\*</sup> The error limits in the extracted diffusive coefficient and the home range size, here and elsewhere in this paper, refer to an estimate of all possible uncertainties. They include, among others, the result of statistical error propagation and differences among the individuals of the population.

a box potential) to represent the return of the rodents to their burrows, we find that the home range size is found not to differ sizably from the box case.

## 2 Trapping webs and the measurement of displacement

The data we analyze in the present study correspond to field work performed in the period from 1994 to 2003, at four sites in the state of New Mexico, USA (Mills et al., 1999). Eleven trapping webs were permanently set at each of the four sites, and animals were captured on a monthly basis for three consecutive nights on each occasion. Several species of *Peromyscus* are present at all sites, of which we chose *P. maniculatus* for this analysis, both because it was the most abundant and because it was the host and reservoir of Sin Nombre virus. Restricting our attention to especially reliable data, we found that the record contained 3765 captures of *P. maniculatus*, corresponding to 1581 animals (794 males, 690 females, and 97 of unidentified gender). The captures consisted mainly of adult animals, but juveniles and sub-adults were captured as well. We performed the analysis only on adults (1108 animals) which were also the ones that were recaptured most. A few young animals were later recaptured as adults, but in general they were captured only once; there is no way to know whether they were transient, or moved away from the current site to establish their home ranges elsewhere, or died sometime after their initial capture event.

The use of trapping webs such as the one schematized in Fig. 1, as well as the analysis of the capture-release-recapture observations, is an implementation of the “distance sampling” method (Buckland, 1993). It is well documented and theoretically sound for the estimation of absolute densities (Parmenter et al., 2003; Anderson et al., 1983). For the study of the movement of the animals, however, the web presents an obvious inconvenience: the distribution of traps is very inhomogeneous. Certainly, it is precisely the inhomogeneity of the design that is responsible for making this method particularly suited for estimating the density at the center of the web. However, this design produces a strong bias in the distribution of distances present in the array, as can be observed in Fig. 2 (heavy line, denoted  $w(r)$ ).

Figure 2 also shows the observed distribution of the displacement of mice at several time intervals, ranging from 1 day to 3 months, compared with the distribution of distances in the web. Since the traps are measured monthly during three consecutive days, we chose to sort the data according to the following time intervals, that we refer to as “time scales”: 1 day, 2 days, and multiples of 30 days. As a result of the logistics of the field work, many of the observed displacements do not correspond exactly to one of these time intervals. We decided to assign those displacements to the closest of the time scales. All the

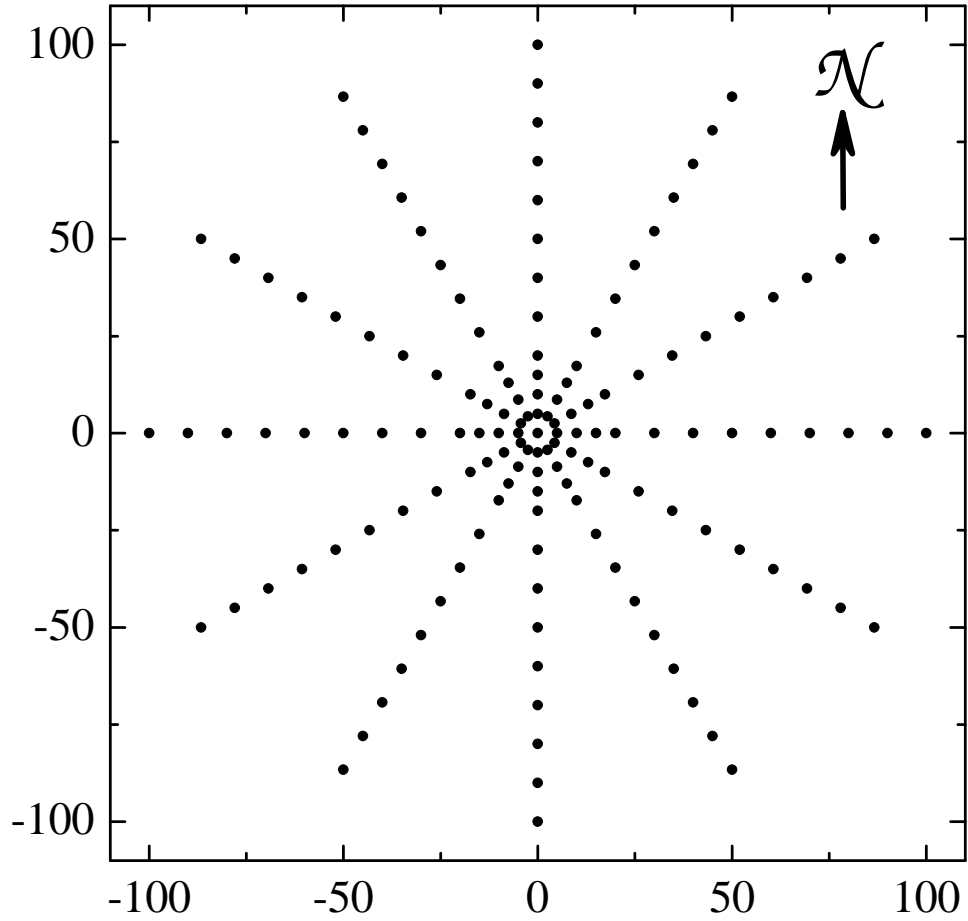


Fig. 1. Arrangement of each of the 11 trapping webs (the arrow represents the North direction). Each dot represents a Sherman trap, except at the center, where there are four traps. The four inner circles have radius increasing in 5 m intervals, while the rest are separated by 10 m. (See (Parmenter et al., 2003) for details.)

observations corresponding to each time scale are pooled together, and the distributions shown in Fig. 2 are their normalized histograms.

It is apparent that, after just two days, the distribution  $q(r)$  develops a deep trough at  $r = 0$ , reflecting the bias of the distances present in the web. If the motion were purely diffusive, and if the measurements of the displacements were fine enough, these distributions should be decreasing Gaussians, always with a maximum at zero. The artifact produced by the web is equivalent to a repulsion at short distances, as if the animals would prefer to stay away from their initial position. This is obviously fictitious. It is necessary to remove this artifact in order to obtain sensible measurements of the motion. Nevertheless, the reader will note that, at 1 day, the distribution of displacements still has a maximum at, or very near, zero. This is an indication that the measurements

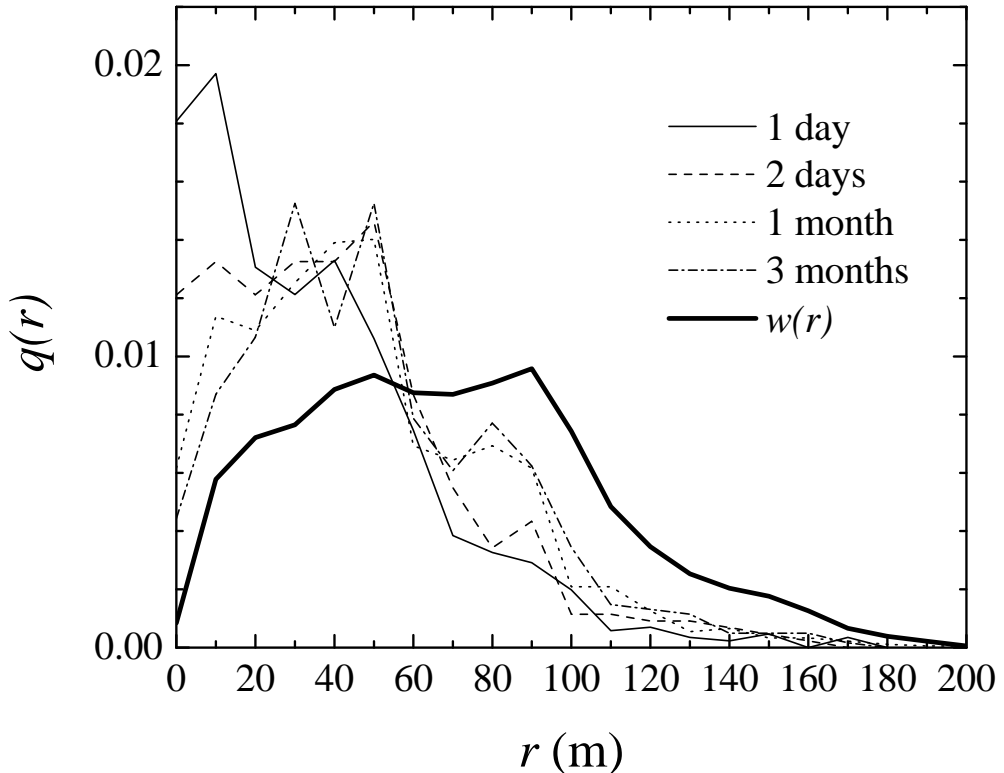


Fig. 2. Observed distribution  $q(r)$  of displacements  $r$  at several time scales, compared with the distribution  $w(r)$  of distances in the web.

on this time scale can be reliably used for the estimation of the diffusion coefficient. Indeed, if one would draw displacements at random, and uniformly, over the web, the observed distribution would be that given by  $w(r)$  in Fig. 2. Random displacements over the web should be expected, for example, if at long times the diffusive movement becomes restricted by the home ranges of the animals. That the distribution at 1 day is far from this shape indicates that, on this time scale, the saturation has not yet been attained.

An alternative view is provided by Fig. 3. It shows the number of distances present in the web in the East-West direction, as well as in two alternative grids (discussed below). The over-sampling of short distances with respect to long distances is very clear: an ideal device to measure displacements should show a square distribution in this picture, homogeneous for all distances up to the diameter of the region being sampled (in the present case, a constant at 0.005, from  $-100$  m to  $100$  m). It is worthwhile to stress that the measurements have been taken with the purpose of monitoring the density and its variations, and not the movement. This longitudinal study is, nevertheless, so unique that it is worthwhile to use it to obtain other demographic parameters such as, in this case, the diffusion ones.

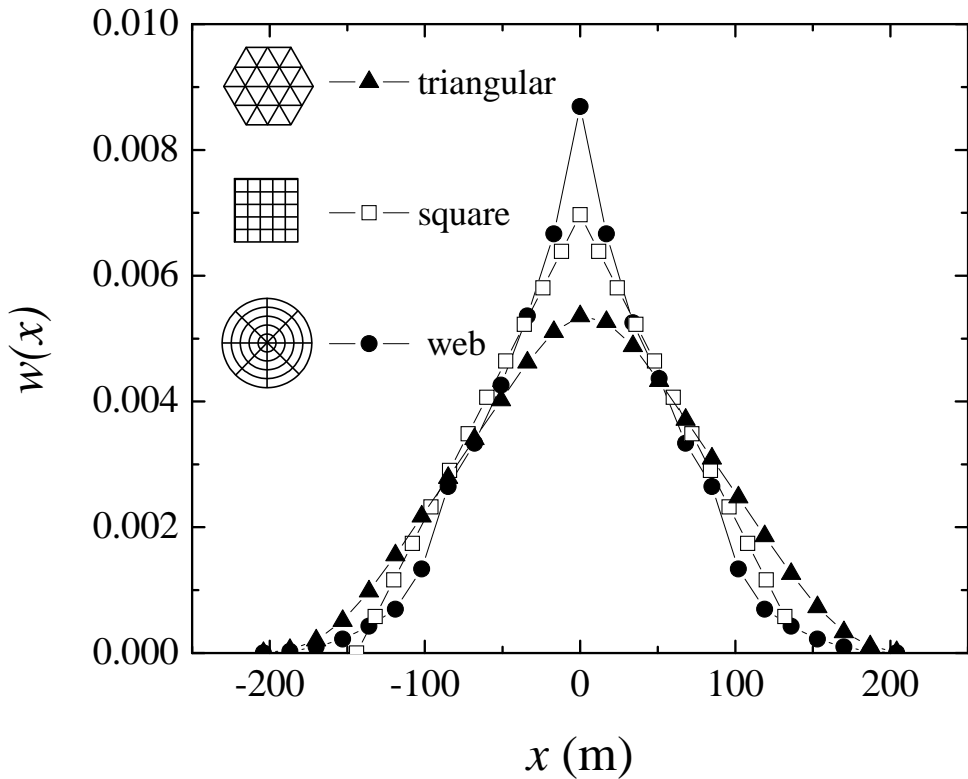


Fig. 3. Distribution of East-West distances in three trapping configurations: a web, a square grid, and a triangular grid (of hexagonal perimeter), schematized in the legend. The diameter of the grids is 200 m in the three cases, and the number of traps as approximately the same as it can be (given the geometries of the designs).

Let us consider alternatives to the web of traps, and how they might affect the measurement of the displacements. Figure 3 shows a comparison of the distribution of distances in the East-West direction for three trapping configurations: a web (as in Fig. 1), a square lattice, and a triangular lattice of hexagonal perimeter (see the simplified diagrams in the legend of Fig. 3.) For the purpose of a sensible comparison, the three configurations have all been taken to have a diameter of 200 m, understood as the longest distance within each configuration, but the number of traps has been taken different in each case. The number selected in each case approximates, as best as possible given the geometrical constraints, the 148 traps used in the webs of Fig. 1: 144 for the square grid, and 127 for the triangular grid. It is easy to see that, of the three, the web has the least homogeneous distribution of distances, with a sharp peak at zero. To quantify this effect, we calculate the fraction  $f$  of distances smaller than one fourth the diameter, viz. 50 m in this case. The results for the three configurations are as follows:

$$f_{\text{web}} = 0.63, \quad f_{\text{sq.}} = 0.56, \quad f_{\text{tr.}} = 0.50.$$

The triangular grid is not only the one with the smallest  $f$  (thus closer to the value a uniform distribution would have) but it also has a flat maximum at zero. A sufficiently large triangular lattice could provide a wide range of distances with a rather flat distribution, and thus could be a better choice for the measurement of displacements. A larger trapping web would comprise, however, more traps and the possibility of its use should be assessed for each intended application.

### 3 Renormalization of the measurements and estimation of the diffusion constants

We use the discussion of the previous section in the analysis of the displacements. Let us consider the displacements of recaptured animals as a statistical ensemble, representing the movement of a hypothetical mouse—henceforth referred to as a “walker”—whose statistical properties we intend to derive from the data. When observed on a short time scale, the motion of the walker might be approximately diffusive. At longer times, both the existence of home ranges and the finiteness of the array should take over, constraining the walk. Other components of the mouse movement, such as explorations and shifting of the home range, might appear as well, but since they are more rare and we are averaging over an ensemble of animals, we restrict ourselves to the consideration of confined diffusive motion.

Supposing that the motion of the mice is indeed diffusive, the probability density function of the displacements of an ensemble of mice from an initial position is just the standard (Gaussian) propagator of diffusive motion, with diffusion coefficients that are generally different in different directions because of anisotropy in the motion. If the motion of the mice could be followed with arbitrary precision, one would expect the mean squared displacement to be linear in time at short times, before saturation takes over to limit the size of the displacements. However, the measurements of position are taken with a discrete device. The corresponding values of the probability density are, therefore, biased. It is possible to take into account the distribution of distances between traps in the web to have the effect of this bias, in the following way. The probability  $Q(x) = q(x)dx$  of observing a displacement between  $x$  and  $x + dx$ , is equal to the probability  $P(x) = p(x)dx$  that, in a day’s time, the walker actually makes such a movement, multiplied by the probability that the web contains such a distance,  $W(x) = w(x)dx$ . We can renormalize the observations to obtain the distribution of displacements that characterized the movement:

$$P(x) = \frac{Q(x)}{W(x)} = \frac{q(x)}{w(x)}. \quad (1)$$

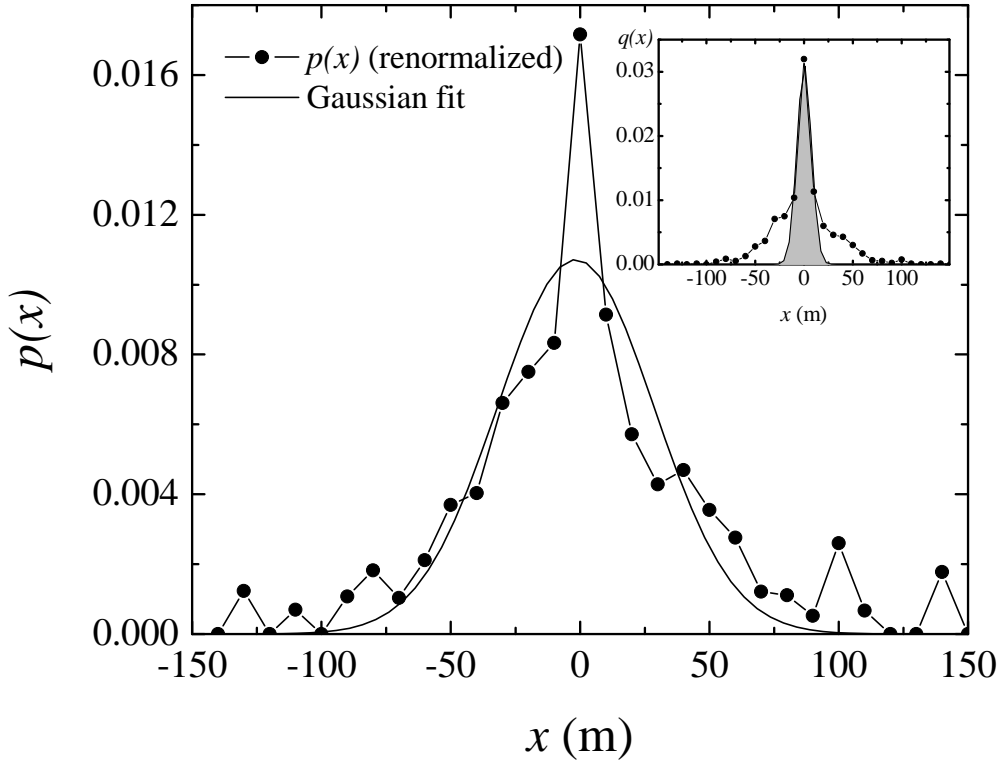


Fig. 4. Distribution of displacements in the East-West direction at 1 day, renormalized with the distribution of distances  $w(x)$ . The continuous line shows the least squares Gaussian fit, and captures well ( $\chi^2 = 1.3 \times 10^{-4}$ ) the width of the distribution. The inset shows the distribution obtained directly from the data, before the renormalization, together with the least squares Gaussian fit (in grey,  $\chi^2 = 2.2 \times 10^{-4}$ ). The “shoulder” arising from the existence of the inner and finer set of traps, and the failure of the Gaussian to represent this shoulder, are both clearly apparent.

The distributions  $q(x)$  and  $w(x)$  can be built from the recapture data and from the geometry of the web, respectively ( $w(x)$  has indeed been shown in Fig. 3). As expected, the distribution  $p(x)$  is bell-shaped, as can be observed in Fig. 4. Moreover, on the 1-day time scale, it is well fitted by a Gaussian ( $\chi^2 = 1.3 \times 10^{-4}$ ), supporting the hypothesis that the movement is initially diffusive. Remarkably, the distribution  $q(x)$ , shown as an inset in Fig. 4, while bell-shaped, cannot be well represented by a Gaussian.

Within the approximation that the movement is initially diffusive, we can identify this Gaussian with the propagator of the diffusion process at 1 day, which is the shortest time scale available from the measurements. The result, in both the  $x$  (East-West) and the  $y$  (North-South) directions, is:

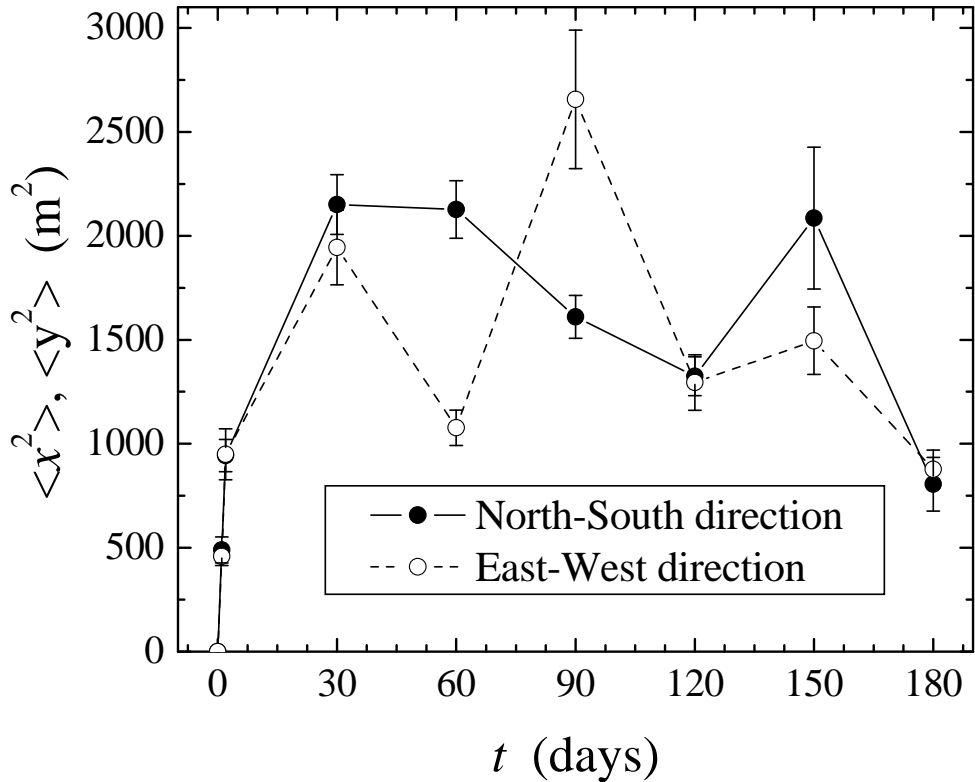


Fig. 5. Mean square displacement as a function of time, in the two directions. The values are calculated as the second moment of the Gaussians fitted to the renormalized distributions of displacements. The initial slope of each curve is  $2Dt$ .

$$D_x = 460 \pm 50 \text{ m}^2/\text{day}, \quad (2)$$

$$D_y = 490 \pm 50 \text{ m}^2/\text{day}, \quad (3)$$

or an average of  $470 \pm 50 \text{ m}^2/\text{day}$ . A typical distance covered diffusively in one day is, thus, of the order of 20 m.

#### 4 Saturation of the mean square displacement and evaluation of home ranges

The analysis described in Section 3 can be carried over at each of the accessible time scales: over a day, two days, and from one month to six months. The result is shown in Fig. 5, where the growth of the mean square displacement of the walker (in both directions) is shown as a function of time. After the initial linear regime the curves saturate (with strong fluctuations due to indeterminancies of the measurements) in both directions to the values

$$\begin{aligned}\langle x^2 \rangle &= 1560 \pm 650 \text{ m}^2, \\ \langle y^2 \rangle &= 1680 \pm 540 \text{ m}^2.\end{aligned}\tag{4}$$

As explained in I, this saturation is the result of a combination of two effects: the existence of home ranges on the one hand and of a spatial window of available observations—provided by the trapping array—on the other. It is easy to envisage two simple models of rodent motion. In one, the existence of the home range is represented by motion that is confined within a finite area but assumed to be otherwise free (and of course diffusive as is appropriate to a random walker). We call this the box model. In the other model the attraction the rodent feels to its burrow is represented by a potential typically continuous in space and the motion is described (Kuperman et al., 2004) by a Fokker-Planck equation (Risken, 1989) instead of the simple diffusion equation. The simple assumption that the potential is harmonic yields what we call the harmonic model.

While we mentioned both these models in our earlier work (Giuggioli et al., 2005a), we used only one of them, the box model, for parameter estimation. The box model procedure to obtain the home range size consists of evaluating the mean square displacement at steady state inside the grid of width  $G$  considering that each captured-recaptured mouse has a home range that could be centered anywhere in space. We perform numerical simulations to represent such a real capture-recapture experiment. A typical simulation consists of randomly taking two positions  $x_0$  and  $x_1$  from a uniform distribution of width  $L$  centered at  $x_c$  in space. Only those values such that the displacement  $x$  is completely contained in the window  $(-G/2, G/2)$  are considered actual observations, and stored for the calculation of the mean square displacement  $\langle x^2 \rangle$ . The mean square displacements are then averaged over the burrow position  $x_c$ , characterizing each mouse. The resultant plot as a function of  $L$  (relative to  $G$ ) is displayed in Fig. 6.

With this procedure it is possible to calculate, with the aid of the simulated result, the value of the home range for *P. maniculatus* in New Mexico. This is shown by the arrows in Fig. 6 to be  $L = 100 \pm 25$  m. This value is a little smaller than those that correspond to the report of Stickel [see (Stickel, 1968), p. 380]. The latter are expressed in units of area: that averages 1.77 ha (with a range from 0.67 to 4.02 ha), for a single observation of *P. m. blandus* during the summer, in a mesquite habitat in New Mexico.

We now ask what the sensitivity of these results is to the assumed square shape of the potential in the box model. If the potential is, instead, harmonic, the simulation procedure changes only with respect to the distribution of initial capture and recapture: it is now Gaussian rather than uniform. To allow a meaningful comparison, we choose the width of the Gaussian distribution as

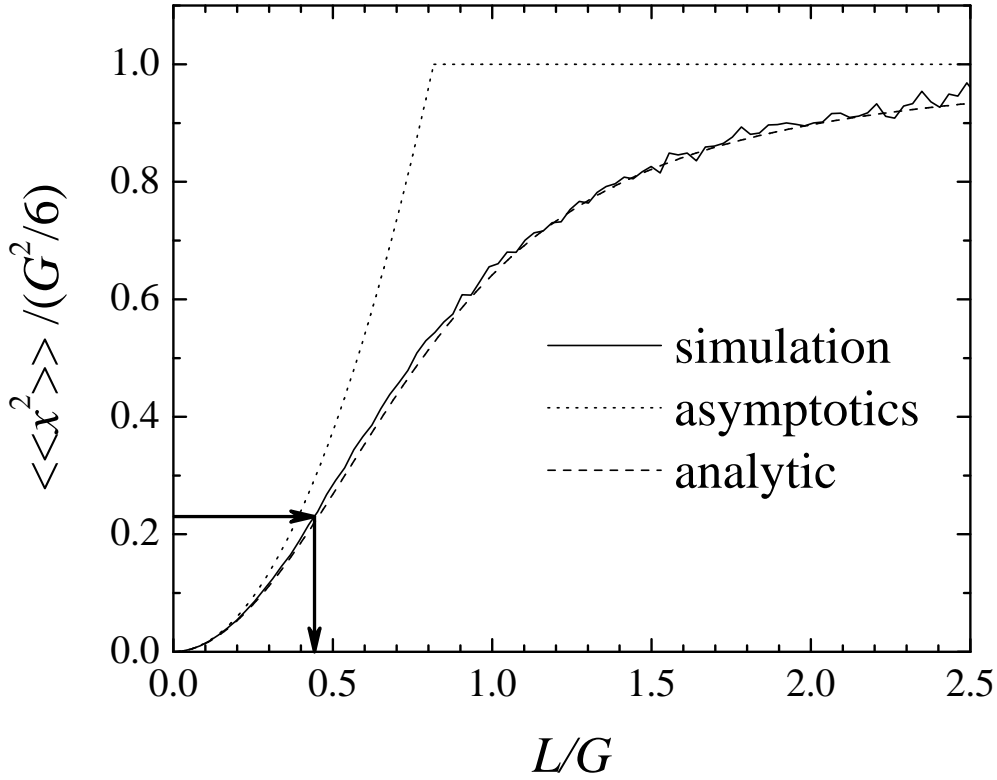


Fig. 6. Simulated mean square displacement for the two potentials, box (solid line) and harmonic (dashed line). The arrows show the value corresponding to the field measurements of *P. maniculatus*, and the consequent value of the home range size, as  $L = 100 \pm 25$  m. The grey lines on the sides of the arrows delimit the error interval. The notation  $\langle\langle x^2 \rangle\rangle$  indicates that an additional average (over the burrow positions  $x_c$ ) has been performed on  $\langle x_{sat}^2 \rangle$  of Eq. (5).

being related to the confining length in the box model in such a way that results of both agree in the limit  $\zeta = G/L \rightarrow +\infty$ . Here  $\zeta$  is the ratio of the grid size  $G$  to the characteristic confining length  $L$ . In the box case  $L$  equals the width of the box. In the harmonic case it is simply related to the curvature of the harmonic potential. In the opposite limit,  $\zeta \rightarrow 0$ , the mean square displacement is the same in both models. The determination of  $L$  for the harmonic model proceeds as follows.

The mean square displacement at long times for a mouse roaming inside its home range, concentric with the grid, is given by the quantity

$$\langle x_{sat}^2 \rangle = \frac{\int_{-G/2}^{G/2} dx_0 \int_{-G/2}^{G/2} dx_1 (x_1 - x_0)^2 \mathcal{P}_{st}(x_0) \mathcal{P}_{st}(x_1)}{\int_{-G/2}^{G/2} dx_0 \int_{-G/2}^{G/2} dx_1 \mathcal{P}_{st}(x_0) \mathcal{P}_{st}(x_1)}, \quad (5)$$

where  $\mathcal{P}_{st}(x) = \exp[-U(x)/D] \left\{ \int_{-\infty}^{+\infty} dx \exp[-U(x)/D] \right\}^{-1}$  is the stationary

distribution of the Fokker-Planck equation for the potential  $U(x)$ . In the harmonic case  $U(x) = \gamma x^2/2$ , and the evaluation of Eq. (5) gives

$$\langle x_{sat}^2 \rangle = \frac{2D}{\gamma} \left[ 1 - \frac{2Ge^{-\frac{G^2}{8D/\gamma}}}{\sqrt{8\pi D/\gamma} \operatorname{erf}(G/\sqrt{8D/\gamma})} \right], \quad (6)$$

which equals  $G^2/6$  when  $G/(D/\gamma) \ll 1$  and  $2D/\gamma$  when  $G/(D/\gamma) \gg 1$ . Requiring that the limit of  $\langle x_{sat}^2 \rangle$  when  $G \rightarrow +\infty$  is equal for both potentials, implies that  $L = \sqrt{12D/\gamma}$ . As a consequence, the stationary distribution for the harmonic model is

$$\mathcal{P}_{st}(x) = \frac{e^{-\frac{x^2}{L^2/6}}}{L\sqrt{\pi/6}}. \quad (7)$$

Using expression (7) we have performed a numerical simulation of the harmonic model, which is shown in Fig. 6 as a dashed line. For the measured mean square displacement (marked with arrows in the plot) the result is practically indistinguishable from that of the box model, as is visually clear from the near-coincidence of the solid and the dashed lines in Fig. 6.

For this set of data we thus see that the results are not particularly dependent on the potential used. It is however important to determine the sensitivity of the predicted mean square displacement to the choice of the model potential in a general way, considering arbitrary potentials, and also carrying out the analysis for temporal evolution as well as for saturation values. We have undertaken such a detailed analysis and its results will be reported elsewhere (Giuggioli et al., 2005b).

## 5 Discussion

Underlying the spatio-temporal behavior of the hantavirus epizootic there are numerous mechanisms, some ecological, some epidemiological, some environmental, and still some of non-biological nature, such as meteorological disruptions like El Niño. The dynamical model (Abramson and Kenkre, 2002) that forms the basis of our recent theoretical investigations (Abramson et al., 2003) requires, for its quantitative application, knowledge of rodent parameters, in particular the diffusion constant. We have set out in I a procedure to evaluate the diffusion constant from recorded rodent movement in grid-based traps and continued that evaluation in the present paper for web-based traps. This latter set of data has been collected from the long term longitudinal study carried out at the University of New Mexico since shortly after the outbreak of HPS, at various places in New Mexico. We have used the displacements of

the mice within the capture webs to derive the statistical properties of their movement. This analysis has provided us not only with an estimation of the diffusion coefficient, but also with information about the home range of the mice.

For our present calculations, the displacement data had to be renormalized with respect to the distribution of distances of the capture web. Indeed, since the webs have been designed to measure absolute densities of the population, and not for the measurement of individual displacement, this distribution is very inhomogeneous. We have shown, however, that it is possible to compensate for this inhomogeneity to obtain a good estimate of the actual distribution of displacements of the population. We have shown, besides, how different geometrical designs of the trapping grid would affect the measurements in different ways.

Extraction of the diffusion constant  $D$  from the short time observations is straightforward, has been explained in I, and yields  $D$  for *P. maniculatus* in New Mexico to be  $470 \text{ m}^2/\text{day}$ , which is larger by a factor of at least 2 relative to the  $D$  deduced in I for *Z. brevicauda* in Panama. This is perhaps in keeping with the expectation that the desert environment requires the mice to move faster and farther to procure the more scant resources.

The observed saturation of the mean square displacement implies the existence of a length scale. There are two separate length scales in the system analyzed. One of them is imposed by the measurement and is the size of the trap region, denoted by  $G$  in our analysis. The other is a true characteristic of the rodent motion, the home range size  $L$ . It is important to distinguish between the effect of these two separate quantities on the observations. Our theoretical studies have shown that the saturation value of the mean square displacement varies in the form of a sigmoidal curve as a function of the ratio  $L/G$ . For grid sizes large with respect to the home range, the mean square displacement varies as the square of the home range while in the opposite limit of small grid size it is proportional to the square of the grid size. Not only is this behavior qualitatively similar for the box model and the harmonic model but the deduced value of the home range is also quantitatively similar as we have shown in Fig. 6. The question of the precise influence that the assumed model potential has on the interpretation poses an interesting theoretical challenge. Our ongoing work on that issue addresses arbitrary potentials and will be reported elsewhere (Giuggioli et al., 2005b).

While the initial purpose of our investigations was the estimation of the diffusion constant of the mice from field observations, the analysis in I as well as in the present paper has also resulted in attention being focused on the concept of home ranges. They have, of course, been known and discussed widely earlier in the literature (Burt, 1943; Stickel, 1968; Anderson, 1982;

Ford, 1974; Wolff, 1989, 2003). Our considerations make clear that it is crucial to incorporate them in descriptions of the spread of epidemics such as the Hantavirus. We are currently working towards the development of a series of new theoretical models for this purpose. One of the underlying ideas in the new models is to consider some of the mice to be largely stationary (moving within their home ranges) and others to be largely itinerant (in search of home ranges of their own) (Kenkre et al., 2004). Another important alternative is to consider the effects of gender on the motion and home ranges (Wolff, 1992, 1997) and of the dependence of the home range size on the density of the rodents (Parmenter and MacMahon, 1983; Wolff, 1984, 2003). We are trying to assess information about such issues from data available to us from the New Mexico observations.

## Acknowledgements

It is a pleasure to thank Aaron Denney for discussions. This work was supported in part by the NSF under grant no. INT-0336343, by NSF/NIH Ecology of Infectious Diseases under grant no. EF-0326757, by the CDC Cooperative Agreement no. USO/CCU613416-01, and by DARPA under grant no. DARPA-N00014-03-1-0900. G. Abramson acknowledges partial funding by CONICET (PEI 6482), and by Fundación Antorchas.

## References

Abramson, G., and Kenkre, V.M., 2002. Spatio-temporal patterns in the Hantavirus infection. *Phys. Rev. E* **66**, 011912-1-5.

Abramson, G., Kenkre, V.M., Yates, T.L., and Parmenter, R.R., 2003. Traveling waves of infection in the Hantavirus epidemics. *Bull. Math. Biol.* **65**, 519-534.

Aguirre, M.A., Abramson, G., Bishop A.R. and Kenkre, V.M., 2002. Simulations in the mathematical modeling of the spread of the Hantavirus. *Phys. Rev. E* **66**, 041908-1-5.

Anderson, D.J., 1982. The home range, a new nonparametric estimation technique. *Ecology* **63**(1), 103-112.

Anderson, D.R., Burnham, K.P., White, G.C. and Otis, D.L., 1983. Density estimation of small-mammal populations using a trapping web and distance sampling methods, *Ecology* **64**, 674-680.

Buckland, S.T., 1993. Distance sampling: estimating abundance of biological populations. Chapman & Hall, London/New York.

Burt, W.H., 1943. Territoriality and home range concepts as applied to mammals. *J. Mammalogy* **24**, 346-352.

Childs, J.E., Ksiazek, T.G., Spiropoulou, C.F., Krebs, J.W., Morzunov, S., Maupin, G.O., Gage, K.L., Rollin, P.E., Sarisky, J., Enscore, R.E., Frey, J.K., Peters, C.J. and Nichol, S.T., 1994. Serologic and genetic identification of *Peromyscus maniculatus* as the primary rodent reservoir for a new hantavirus in the southwestern United States. *J. Inf. Dis.* **169**, 1271-1280.

Ford, R.G., 1974. The analysis of space use patterns. *J. Theor. Biol.* **76**, 125-155.

Giuggioli, L., Abramson, G., Kenkre, V.M., Suzán, G., Marcé, E. and T.L. Yates, 2005a. Diffusion and home range parameters from rodent population measurements in Panama. *Bull. Math. Biol.* in press.

Giuggioli, L., Abramson, G. and Kenkre, V.M., 2005b. Theory of home range estimation from displacement measurements of animal populations. *J. Theor. Biol.* submitted.

Kenkre, V.M., Abramson, G., Giuggioli, L., Camelo Neto, G., 2005. Theory of Hantavirus infection spread incorporating localized adults and itinerant juvenile mice. University of New Mexico preprint.

Kuperman, M. N. and Kenkre, V. M., 2004. Spatial features of population dynamics, effects of mutual interactions and of interaction with the environment. Preprint.

Mills, J.N., Yates, T.L., Ksiazek, T.G., Peters, C.J. and Childs, J.E., 1999. Long-Term Studies of Hantavirus Reservoir Populations in the Southwestern United States: Rationale, Potential, and Methods. *Emerging Infectious Diseases* **5**, 95-101.

Murray, J.D., 1993. Mathematical Biology, 2nd edition. Springer, New York.

Nichol, S.T., Spiropoulou, C.F., Morzunov, S., Rollin, P.E., Ksiazek, T.G., Feldmann, H., Sanchez, A., Childs, J., Zaki, S. and Peters, C.J., 1993. Genetic identification of a hantavirus associated with an outbreak of acute respiratory illness. *Science* **262**, 914-197.

Okubo, A., 1979. Diffusion and ecological problems: mathematical models. Springer-Verlag, Berlin.

Parmenter, R.R., MacMahon, J.A., 1983. Factors determining the abundance and distribution of rodents in a shrub-steppe ecosystem: the role of shrubs. *Oecologia* **59**, 145-156.

Parmenter, R.R., Yates, T.L., Anderson, D.R., Burnham, K.P., Dunnum, J.L., Franklin, A.B., Friggens, M.T., Lubow, B.C., Miller, M., Olson, G.S., Parmenter, C.A., Pollard, J., Rexstad, E., Shenk, T.M., Stanley T.R. and White, G.C., 2003. Small-mammal density estimation: a field comparison of grid-based vs. web-based density estimators. *Ecological monographs* **73**, 1-26.

Risken, H., 1989. The Fokker-Planck equation : methods of solution and applications. Springer-Verlag, New York.

Stickel, L.F., 1968. Home Range and Travels. In: King, J.A. (editor), *Biology of Peromyscus (Rodentia)*, Special Publication No. 2, The American Society of Mammalogists, Stillwater, OK, pp. 373-411.

Terman, C.R., 1968. Population dynamics. In: King, J.A. (editor), *Biology of*

Peromyscus (Rodentia), Special Publication No. 2, The American Society of Mammalogists, Stillwater, OK, pp. 412-450.

Vessey, S.H., 1987. Long-term population trends in white-footed mice and the impact of supplemental food and shelter. *Am. Zoologist* **27**, 879-890.

Wolff, J.O., 1984. The effects of density, food, and interspecific interference on home range size in *Peromyscus leucopus* and *Peromyscus maniculatus*. *Can. J. Zool.* **63**, 2657-2662.

Wolff, J.O., 1989. Social behavior. In: Kirkland Jr., G. L. et al. (Eds.), *Advances in the study of Peromyscus (Rodentia)*, Texas Tech University Press, Lubbock, TX, pp. 271-291.

Wolff, J.O., 1992. Parents suppress reproduction and stimulate dispersal in opposite-sex juvenile white-footed mice. *Nature* **359**, 409-410.

Wolff, J.O., 1997. Population regulation in mammals: an evolutionary perspective. *J. Animal Ecol.* **66**, 1-13.

Wolff, J.O., 2003. Density-dependence and the socioecology of space use in rodents. In: Singleton, G.R. et al. (Eds.), *Rats, mice and people: Rodent biology and management*, ACIAR monograph No. 96, pp. 124-130.